Pergamon

0025-5408(95)00176-X

ELECTRICAL PROPERTIES OF Cu₂P₃I₂

Eva Freudenthaler[1], Arno Pfitzner[1] and Derek C. Sinclair[2]
[1] Universität-Gesamthochschule Siegen, Anorganische Chemie,
57068 Siegen, Germany
[2] University of Aberdeen, Department of Chemistry, Meston Walk,
Aberdeen, Scotland AB9 2UE

ABSTRACT

Conductivity data on single crystal and cold-pressed polycrystalline samples of $Cu_2P_3I_2$ demonstrate that Cu^+ ion migration dominates the electrical conductivity over the temperature range 25-300°C in argon. Both sets of samples exhibit fully reversible Arrhenius-type conductivity behavior with activation energy values of ~0.45eV and typical conductivity values of ca. 1.90 × 10^{-3} S.cm^{-1} at 186°C. The conductivity appears to be one-dimensional.

KEYWORDS: A. inorganic compounds, C. impedance spectroscopy, D. electrical properties

INTRODUCTION

Until the recent discovery of $(CuI)_3P_{12}$ (1) and $Cu_3P_{15}I_2$ (2), the compound $Cu_2P_3I_2$ (3) was the only known ternary phase in the Cu-P-I system. The crystal structure of $Cu_2P_3I_2$ is dominated by one-dimensional, infinite chains of covalently bonded phosphorus atoms which are surrounded by Cu^+ and I^- ions, as shown in Figure 1. In the unit cell there are 32 Cu^+ ions distributed over 60 atomic positions with site occupancies ranging from 15 to 97 ± 1% (3). Given that the crystal structure shows one-dimensional channels and a lot of vacancies in the copper sub-lattice, it would appear reasonable that $Cu_2P_3I_2$ should exhibit enhanced Cu^+ ion mobility. This hypothesis is supported by the fact that $Cu2P_3I_2$ undergoes ion exchange in aqueous $AgNO_3$ to form the isotypic silver compound, $Ag_2P_3I_2$ (3).

Electrical data on $Cu_2P_3I_2$ are limited. Möller reported (4) Arrhenius-type conductivity behavior for cold pressed pellets of $Cu_2P_3I_2$ between copper electrodes from dc measurements. Due to electrode contact problems, however, no specific conductivity values

FIG. 1.

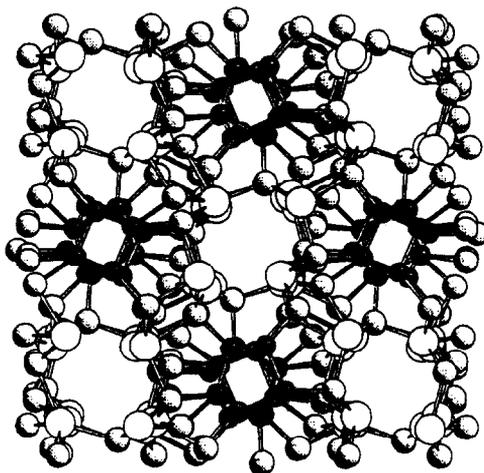Crystal structure of $Cu_2P_3I_2$ viewed along the phosphorus chains. The filled, shaded and empty spheres correspond to phosphorus, copper and iodine atoms, respectively. The unit cell is monoclinic (3).

were calculated. In this paper, we report specific conductivity values for single crystal and polycrystalline samples of $Cu_2P_3I_2$ using ac impedance spectroscopy.

EXPERIMENTAL

Needle-like single crystals of $Cu_2P_3I_2$ were obtained via chemical transport in evacuated silica tubes from stoichiometric quantities of CuI (Aldrich, 99.999%) and red phosphorus (Mining and Chemical Products Ltd., 99.999+%). A small excess of iodine was added to promote vapor phase transport. The reaction was carried out at 500°C for 39 days. Typical crystal dimensions were (2-5)mm $\times$ 10^{-4} cm^2 (length $\times$ cross-sectional area). Further details of the crystal growing procedure are given elsewhere (5).

   Due to the mechanical instability of the needle-shaped crystals, it was necessary to embed them in an epoxy matrix so that electrodes could be applied to the crystals with minimal damage. Crystals selected for electrical measurements were washed in acetone to remove traces of iodine and phosphorus iodides. They were placed in a small mold filled with epoxy resin which was initially cured at 25°C and then at 60°C. The resin block was cut using a diamond saw to expose opposite ends of the needle axis, with a needle length of ca. 8mm inside the block. After measuring the cross-sectional area of the crystals under a light microscope, the crystal end-faces were sputtered with gold. Although it was not possible to restrict the gold coverage to the cross-sectional area of the crystals, attempts were made to keep spill-over small so as to minimize any ac response from the epoxy resin during measurements. Several attempts at embedding, cutting and electroding crystals were required before a suitable sample was prepared for ac impedance measurements.

Powder of $Cu_2P_3I_2$ was prepared via solid state reaction of stoichiometric quantities of CuI powder and small pieces of red phosphorus in evacuated silica tubes. The reaction was carried out at 500°C for 49 days and the resulting powder was phase-pure by X-ray diffraction. Pellets suitable for electrical measurements were made by cold pressing $Cu_2P_3I_2$ powder in a 10mm stainless steel die with an applied pressure of ca. $2500kg.cm^{-2}$. Gold electrodes were sputtered on opposite sides of the pellets.

The electroded samples (both crystals and pellets) were placed in a spring-loaded conductivity jig in contact with strips of Au foil which were attached to the Pt measuring leads. The jig was placed in a vertical tube furnace, with a thermocouple in close proximity to the sample; temperature was controlled and measured to within 3°C. In order to avoid oxidation of the samples, the atmosphere in the jig was controlled. High purity argon gas (99.998%) was flushed through a silica gel/calcium chloride column to remove moisture and then through a heated silica tube (400°C) containing copper net to remove traces of oxygen before passing over the conductivity jig.

All ac impedance measurements were made with a Solartron 1250 Frequency Response Analyzer/1286 or 1287 Electrochemical Interface and a Hewlett-Packard 4192A Impedance Analyzer. Applied voltages were 100mV and the measured frequency range was 30mHz to 13MHz. The blank parallel capacitance of the conductivity jig was measured and the appropriate corrections were made to the experimental data. Relative permittivity values of $Cu_2P_3I_2$ were calculated using the equation $\varepsilon_r = C'/C_o$, where C' and C_o represent the cell capacitance values with and without the sample, respectively. The leakage resistance of the jig was $>>100M\Omega$ and was much greater than that of the sample at all temperatures studied. The resistance of the electrode leads was $<1\Omega$ and was too small to influence the impedance data.

RESULTS AND DISCUSSION

Conductivity values were extracted from complex impedance plane plots. Typical impedance data are shown in Figure 2 for a polycrystalline sample, (a), and for a single crystal with the applied field parallel to the needle axis, (b).

Pelleted Samples. Figure 2(a) shows three effects, that is, two overlapping arcs and a low frequency inclined spike. Semi-circular arcs are usually represented by resistance and capacitance elements placed in parallel. In the frequency domain, RC elements are characterized by the relationship $\omega_{max}RC = 1$ which holds at the frequency of the maximum loss, ω_{max} (i.e., at arc maxima), in the impedance spectrum. Different RC elements are separable if ω_{max} values differ by >1 decade. It is usually possible to identify different RC elements, based on the capacitance values (6), and assign them to appropriate regions of the sample/electrode configuration.

The higher frequency arc in Figure 2(a) has an associated capacitance of 2×10^{-12} $F.cm^{-1}$. This value is a typical bulk or intra-granular value for a non-polar solid (6) since $\epsilon_r = C'/C_o$ $= 2 \times 10^{-12}/8.8 \times 10^{-14} = 23$. This higher frequency arc, which dominates the impedance spectra, is therefore attributed to the intra-granular response of the pelleted samples. The lower frequency arc has an associated capacitance of 7×10^{-11} $F.cm^{-1}$. This is a typical grain boundary value for porous pellets (~85% theoretical density) where there is poor inter-granular contact.
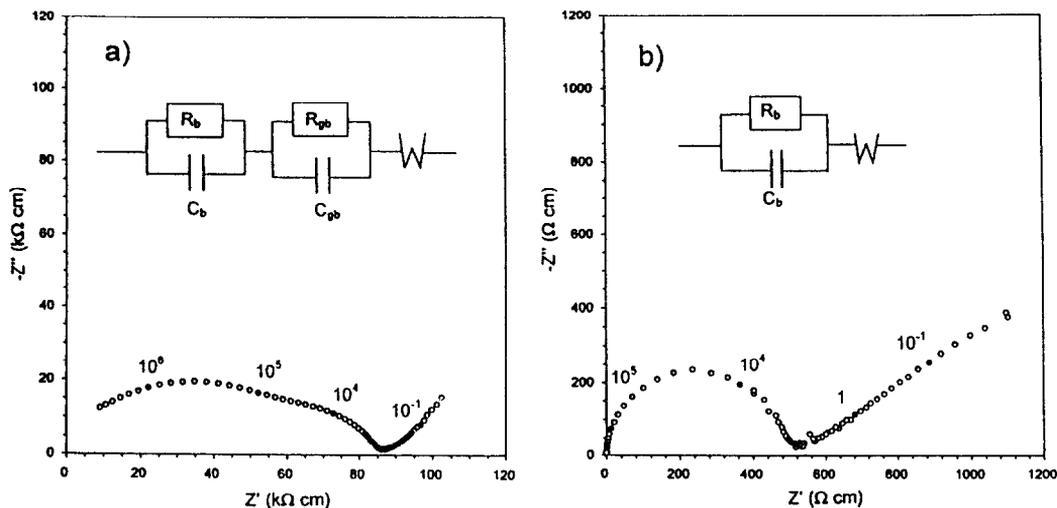
FIG. 2.

Typical complex impedance plane plots for (a) a polycrystalline sample at 72°C and (b) a single crystal at 186°C. Selected frequencies, in Hz, are marked. The inserts show the equivalent circuits used to interpret the impedance data. R_b and R_{gb} correspond to bulk and grain boundary resistances, respectively and C_b and C_{gb} refer to bulk and grain boundary capacitances.

In general, the low frequency response in the Z^* plane provides information regarding the nature of the predominant charge carriers responsible for electrical conduction. In particular, for samples coated with gold electrodes the presence or absence of a low frequency spike in the Z^* plane indicates ionic or electronic conduction, respectively.

The low frequency spike represents charge build-up which arises for ionic conducting samples because the mobile charge carriers are unable to cross the sample/electrode interface. Unless Schottky barriers (7) are developed, there is no such impedance barrier to charge transfer at the sample/electrode interface for electronically conducting materials and therefore there is no sign of a low frequency electrode spike in the Z^* plane.

A sample/electrode interface which has no charge transfer is modeled by an ideal capacitor (8). The associated capacitance for such a completely blocking electrode is calculated by applying the equation $Z'' = 1/\omega C$ to data on the vertical spike; typical capacitance values are 10^{-5} to 10^{-6} F.cm^{-2}.

In practice, most electrodes are partially blocking, that is, there is finite or infinite diffusion of mobile charge carriers into the electrode. This results in an inclined low frequency spike of angle ca. 30-90°, in the complex impedance plane. An inclined spike of angle 45°, involving infinite diffusion, is commonly referred to as a Warburg-type response and is represented by the symbol W in equivalent circuit analysis (Fig. 2).

The Z^* plots for $Cu_2P_3I_2$ clearly show the presence of a low frequency spike with an associated capacitance of ca. 10^{-5} F.cm^{-2} over the measured temperature range (Fig. 2). The low frequency spike is attributed to electrode-sample interfacial impedances which are associated with ionic polarization and diffusion-limited phenomena at the electrode. The inclined spike at an angle of 53° to the real axis is similar to that expected for a Warburg

impedance with an ideal slope of 45°. The presence of this low frequency spike supports the idea that conduction is mainly by means of ions.

The low frequency intercept of the combined arcs gives the total pellet resistance. Extraction of bulk resistance values from the intercept of the higher frequency arc on the real, Z', axis proved difficult, especially at higher temperatures. This was due to poor resolution of the bulk and grain boundary arcs. Only total resistance values, R_T, for polycrystalline samples were extracted; net conductivity data ($\sigma_T = 1/R_T$) of two pellets are shown in Figure 3. Data for both samples showed excellent reproducibility on thermal cycling and good agreement between the two pellets. Reliable conductivity data at temperatures in excess of ca. 280°C could not be obtained due to irreversible chemical reactions between the sample and gold electrodes.

Single Crystals. Several experimental restrictions limited the amount of conductivity data obtainable for the single crystals of $Cu_2P_3I_2$. First, the needle-like shape of the crystals limited electrode configurations such that it was possible to apply electrodes only perpendicular to the needle axis. No quantitative information could therefore be obtained on the conductivity in the other crystallographic orientations. Second, electrodes applied perpendicular to the needle axis resulted in large resistance values because of the long path length and very small cross-sectional electrode area. The resistance of the crystals below 100°C in this orientation exceeded the measuring limit of the electrical apparatus and thus restricted the lowest measuring temperature to ca. 120°C. Third, embedding crystals in epoxy resin restricted the upper measuring temperature to ca. 200°C. Above this temperature, the resin became increasingly elastic and its conductivity became significant. These experimental constraints resulted in a narrow measuring temperature range, that is, 120-200°C for single crystals.

A typical complex impedance plane plot for a single crystal with the field applied parallel to the needle axis is shown in Figure 2(b). A bulk arc and a low frequency electrode spike with an associated capacitance of ~10^{-6} F.cm^{-2} were observed in the complex impedance plane.

Comparison of Single Crystal and Pelleted Samples Data Sets. Single crystal conductivity values are ca. three times higher than the net pellet conductivities, as shown in Figure 3. Differences in the measured conductivity values can be rationalized partly by the fact that values for the polycrystalline samples contain both intra- and inter-granular contributions whereas the single crystal data contain only an intra-granular contribution (Fig. 2). Furthermore, single crystal data are measured along the crystallographic orientation which is probably the most favorable for long range Cu^+ ion migration whereas the polycrystalline samples consist of randomly oriented crystallites. The conductivity of the pellets will therefore be reduced due to the tortuosity in current path.

We are unable to quantify the level of electronic conductivity in $Cu_2P_3I_2$ for the various crystallographic orientations using ac impedance spectroscopy. The presence of a low frequency spike in all Z* plots clearly indicates that the electrical properties of $Cu_2P_3I_2$ are dominated by ionic conduction. Data from the polycrystalline samples indicate that electronic conductivity, in any crystallographic orientation, must be lower than the ionic conduction along the needle axis over the measured temperature range. If this were not the case, it is difficult to explain the presence of a low frequency spike in the Z* plane plots for the polycrystalline samples.
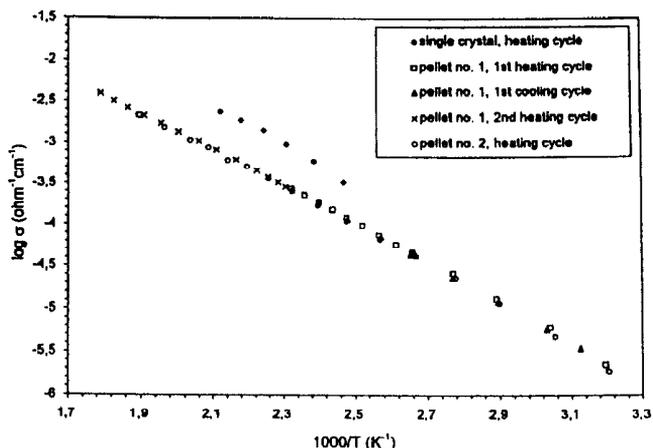
FIG. 3.

Conductivity data for two polycrystalline samples and a single crystal of $Cu_2P_3I_2$.

In conclusion, we have measured for the first time the specific conductivity of $Cu_2P_3I_2$ along the needle direction. The results are consistent with the hypothesis that $Cu_2P_3I_2$ exhibits enhanced Cu^+ ion mobility parallel to the needle axis.

ACKNOWLEDGMENTS

REFERENCES

1. A. Pfitzner and E.Freudenthaler, Angew. Chem., in press.
2. A. Pfitzner and E.Freudenthaler, Z. Kristallogr. **210**, 95 (1995).
3. M.H. Möller and W. Jeitschko, J. Solid State Chem. **65**, 178 (1986).
4. M.H. Möller, Dissertation, Universität Dortmund (1983).
5. E. Freudenthaler, Dissertation, Universität Siegen (1996).
6. J.T.S Irvine, D.C. Sinclair and A.R. West, Adv. Mater. **2**, 132 (1990).
7. S.N. Sze, Semiconductor Devices, Physics and Technology, Wiley, New York (1985).
8. R.D. Armstrong, J. Electroanal. Chem. **52**, 413 (1974).